# An Analytical Technique for Studying the Anomalous Roll Behavior of Re-Entry Vehicles

FRANK J. BARBERA*
*Kaman Sciences Corporation, Colorado Springs, Colo.*

**Anomalous roll behavior of a spinning re-entry vehicle is examined in detail for the case of a vehicle having a simple compound asymmetry consisting of a lateral center-of-gravity offset combined with an aerodynamic trim angle of attack. The analysis is made utilizing a fast analytical roll response program developed from the linearized equations of motion of a spinning vehicle. The results show that persistent roll resonance is obtained at first resonance with the minimum aerodynamic asymmetry if the asymmetry creates a trim force that lies in-plane with the center-of-gravity offset. A criterion is developed which defines this minimum in-plane aerodynamic asymmetry for the special case of a constant flight-path entry into an exponential atmosphere with constant aerodynamic coefficients. A suggested method of treating Mach-number-dependent aerodynamic coefficients is also presented. Selected six-degree-of-freedom trajectory calculations are used to verify important analytical results.**

## Nomenclature

$C_A$ = axial force coefficient
$C_m, C_n$ = pitching and yawing moment coefficients
$C_{m_q}$ = pitch damping derivative, $\partial C_m/\partial(qd/2V)$, rad$^{-1}$
$C_{m\alpha}$ = pitching moment derivative, $\partial C_m/\partial\alpha$, rad$^{-1}$
$C_{N\alpha}$ = normal force derivative, $\partial C_N/\partial\alpha$, rad$^{-1}$
$d$ = reference length for aerodynamic coefficients, ft
$D,E$ = functions defined by Eqs. (5) and (6)
$F_0$ = force normal to body centerline at $p = 0$, lb
$F_z$ = aerodynamic force along the $Z$ axis, lb
$G_1,G_2,G_3$ = constants of differential equation for $\delta$ [Eqs. (2–4)]
$g_N$ = lateral load factor
$h$ = altitude, ft
$H$ = function defined by Eq. (7)
$i$ = $(-1)^{\frac{1}{2}}$
$I$ = pitch and yaw moment of inertia, slug-ft$^2$
$I'$ = $I/q_\infty Sd$, sec$^2$
$I_x$ = roll moment of inertia, slug-ft$^2$
$l_x$ = aerodynamic moment about the $X$ axis, ft-lb
$m$ = mass of vehicle, slugs
$m'$ = $mV/q_\infty S$, sec
$p,q,r$ = angular rates about the $X,Y,Z$ axes, rad/sec
$p_{cr}$ = critical frequency, rad/sec
$\Delta p$ = change in roll rate from initial condition, rad/sec
$q_\infty$ = dynamic pressure, $\rho_\infty V^2/2$, psf
$R$ = trim amplification factor
$S$ = reference area for aerodynamic coefficients, ft$^2$
$t$ = time, sec
$V$ = relative velocity, fps
$W$ = vehicle weight, lb
$X,Y,Z$ = principal axes (Fig. 1)
$\Delta\lambda$ = static margin (positive for statically stable vehicle), ft
$\Delta Y_{c.g.}$ = center-of-gravity offset along $Y$ axis, ft
$\alpha,\beta$ = body-fixed angles of attack and sideslip, rad
$\alpha_T,\beta_T$ = rolling trim angles of attack and sideslip, rad
$\gamma$ = flight-path angle, deg or rad
$\delta$ = total angle of attack, rad; for $\delta'_0$, see Eq. (23)
$\delta_T$ = total rolling trim angle of attack, rad
$\eta$ = atmospheric scale height, ft$^{-1}$
$\lambda$ = roll rate ratio
$\mu$ = damping ratio
$\xi$ = function defined by Eq. (29)
$\rho_{sl}$ = sea level atmospheric density, slugs/ft$^3$
$\rho_\infty$ = atmospheric density, slugs/ft$^3$
$\varphi$ = windward meridian (Fig. 1), deg or rad; for $\varphi'_0$, see Eq. (24)
$\Delta\varphi$ = shift in $\varphi$ due to roll rate (Fig. 1), deg or rad

***Subscripts***

cr = critical value
$i$ = initial conditions at re-entry
min = minimum value
0 = trim conditions at $p = 0$
res = conditions at resonance

Presented as Paper 69-103 at the AIAA 7th Aerospace Sciences Meeting, New York, January 20–22, 1969; submitted February 3, 1969; revision received June 20, 1969.

* Research Scientist.

## Introduction

ANOMALOUS roll behavior of spinning re-entry vehicles has been observed for years from flight test results of numerous vehicles. Examples of such roll behavior must include: 1) transient roll resonance, 2) roll speed-up then slow-down, 3) roll slow-down then speed-up, 4) transient roll lock-in and breakout, and 5) persistent roll resonance (lock-in). Excellent descriptions of such roll behavior are available in the literature.[1,2]

The importance of first resonance to the initiation of unusual roll behavior has been well established by Nicolaides[1] and other analysts studying roll phenomenology. This paper is primarily devoted to that portion of the re-entry flight immediately preceding, during, and subsequent to first resonance. A parametric analysis is presented for the case of a typical re-entry vehicle having a simple compound asymmetry consisting of a lateral center-of-gravity offset and a trim angle of attack. An efficient computer program, based on the analytical solution of the linearized equations of motion of a rolling vehicle, is used. A criterion is developed for estimating the minimum in-plane compound asymmetry needed for first resonance lock-in. This criterion shows the relative importance of the trajectory parameters, the vehicle mass characteristics, and the configurational characteristics expressed through the aerodynamic coefficients.

## Analysis

The linearized equations of motion for a rolling, symmetrical vehicle having slight aerodynamic asymmetries were derived by Nelson[3] for a body axis system. The assumptions made by Nelson include: 1) the pitch and yaw moments of inertia are equal, 2) the rolling velocity is constant,

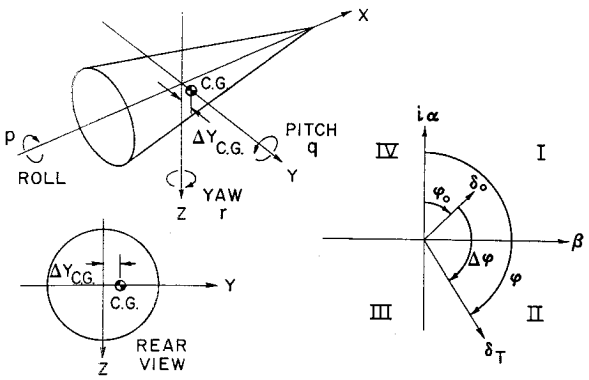


**Fig. 1 Coordinate system and nomenclature.**

3) small $\alpha$ and $\beta$ and linear aerodynamics, 4) a constant axial component of velocity, and 5) the force of gravity and magnus moments are negligible. Nelson's equations were subsequently simplified by Pettus[4] by: 1) introducing trim moments, 2) neglecting trim forces, and 3) neglecting products of aerodynamic derivatives.

The equation for the total angle of attack obtained by Pettus is of the form

$$\ddot{\delta} + G_1\dot{\delta} - G_2\delta = G_3; \quad \delta = \beta + i\alpha \tag{1}$$

where

$$G_1 = \frac{C_{N\alpha}}{m'} - \frac{C_{m_q}d}{2VI'} + ip\left(2 - \frac{I_x}{I}\right) \tag{2}$$

$$G_2 = D - iE \tag{3}$$

$$G_3 = -H + iC_{m_0}/I' \tag{4}$$

$$D = \frac{C_{m\alpha}}{I'} + p^2\left(1 - \frac{I_x}{I}\right) \tag{5}$$

$$E = p\left[\frac{C_{N\alpha}}{m'}\left(1 - \frac{I_x}{I}\right) - \frac{C_{m_q}d}{2VI'}\right] \tag{6}$$

$$H = (C_{n_0}d - C_A\Delta Y_{c.g.})/I'd \tag{7}$$

The sign of $C_{n_0}$ in Eq. (7) differs from that shown by Pettus in Ref. 4, and $C_x$ has been replaced by $C_A$, along with the required change in sign.

The particular solution of Eq. (1) yields the total trim angle of attack

$$\delta_T = \beta_T + i\alpha_T = -G_3/G_2 \tag{8}$$

Substituting for $G_2$ and $G_3$ using Eqs. (3) and (4), carrying through the algebra, and separating the equation into its real and imaginary parts, we arrive at the following expressions for the trim angle of attack and sideslip:

$$\alpha_T = (EH - DC_{m_0}/I')/(D^2 + E^2) \tag{9}$$

$$\beta_T = (DH + EC_{m_0}/I')/(D^2 + E^2) \tag{10}$$

The nonrolling trim angle of attack and sideslip can be obtained from Eqs. (9) and (10) by setting $p = 0$, which yields

$$\alpha_0 = -C_{m_0}/C_{m\alpha} \tag{11}$$

$$\beta_0 = (C_{n_0}d - C_A\Delta Y_{c.g.})/C_m\, d \tag{12}$$

The total nonrolling trim angle is shown schematically in Fig. 1, and its magnitude and orientation are given by

$$|\delta_0| = (\alpha_0^2 + \beta_0^2)^{1/2} \tag{13}$$

$$\varphi_0 = \tan^{-1}(\beta_0/\alpha_0) \tag{14}$$

The magnitude and orientation of the nonrolling trim angle is modified by the roll frequency of the vehicle. This is most clearly demonstrated by determining the ratio of the rolling trim angle to the nonrolling trim angle (trim amplification factor) $R$, which can be shown to be

$$R = \left(\frac{1 - \lambda^2}{(1 - \lambda^2)^2 + (2\mu\lambda)^2}\right) - i\left(\frac{2\lambda\mu}{(1 - \lambda^2)^2 + (2\mu\lambda)^2}\right) \tag{15}$$

where

$$\lambda = p/p_{cr} \tag{16}$$

$$\mu = \rho_\infty^{1/2}\left(\frac{C_{N\alpha}S}{4m} - \frac{C_{m_q}Sd^2}{8(I - I_x)}\right)\left(\frac{-C_{m\alpha}Sd}{2(I - I_x)}\right)^{-1/2} \tag{17}$$

$$p_{cr} = [-C_{m\alpha}q_\infty\, Sd/(I - I_x)]^{1/2} \tag{18}$$

The critical roll frequency $p_{cr}$ is nearly identical to the undamped lateral oscillation frequency, differing only in the roll moment of inertia term appearing in the denominator of Eq. (18).

The magnitude of the trim amplification factor may be written

$$|R| = [(1 - \lambda^2)^2 + (2\mu\lambda)^2]^{-1/2} \tag{19}$$

and its orientation to the nonrolling trim vector (see Fig. 1) is

$$\Delta\varphi = \tan^{-1}[2\lambda\mu/(1 - \lambda^2)] \tag{20}$$

The magnitude of the rolling trim vector is given by $|\delta_T| = |R|\ |\delta_0|$, and the proper quadrant for $\Delta\varphi$, with respect to $\delta_0$, is determined by monitoring the sign of $\sin\Delta\varphi$ and $\cos\Delta\varphi$.

### Analytical Roll Response Program

The equations of the previous section have been incorporated into a point-mass trajectory program, which utilizes Mach number dependent aerodynamic coefficients, to form a fast analytical roll response program. The rolling trim angles of attack and sideslip are given by $\alpha_T = |\delta_T|\cos\varphi$ and $\beta_T = |\delta_T|\sin\varphi$, respectively, where $\varphi = \varphi_0 + \Delta\varphi$.

Since the center-of-gravity offset has been selected along the $Y$ body axis, only the $\alpha_T$ component of the rolling trim vector can furnish a rolling torque, which is given by

$$l_x = C_{N\alpha}(\alpha_T\Delta Y_{c.g.})q_\infty S \tag{21}$$

The roll acceleration is given by $\dot{p} = l_x/I_x$, from which the roll history is easily evaluated using numerical integration. The lateral load factor is given by

$$g_N = C_{N\alpha}|\delta_T|q_\infty S/W \tag{22}$$

Neglecting minor oscillatory perturbations, the long-term roll-rate change throughout the trajectory is dependent only upon the trim history of the vehicle. Numerous comparisons of the results obtained with the roll response program and 6-DOF calculations have established the accuracy of the

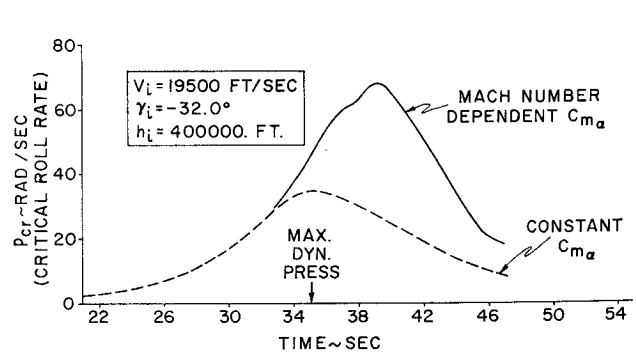


**Fig. 2 Variation of the critical roll rate with time.**

analytical method for computing $\delta_T$, $\alpha_T$, $\beta_T$, $g_N$, and $p$. On the average, a 6-DOF simulation will take ~200 times as long as a similar calculation with the analytical roll program.

### Roll Response Analysis

The roll response of a small re-entry vehicle to a wide range of trim moment coefficients was determined using the foregoing program. The initial re-entry conditions and hypersonic aerodynamic coefficients considered for the analysis are as follows:

$V_i$ = 19,500 fps, $\gamma_i = -32.0°$

$h_i$ = 400,000 ft, $\alpha_i = =0.3°$, $\beta_i = o°$

$p_i$ = 12.56, $q_i = o$, $r_i = 0.07$ rad/sec

$C_A$ = 0.120, $C_N$ = 0.670 rad$^{-1}$, $C_{m_\alpha} = -0.0208$ rad$^{-1}$

$C_{m_q} = -0.95$ rad$^{-1}$, static margin = 3.1% length

The center-of-gravity displacement was kept constant at 0.0025 ft along the positive $Y$ axis of the vehicle, but the results are applicable to any other displacement orientation by a simple rotation of the axes. The study was made using Mach-number-dependent aerodynamic coefficients.

The variation of $p_{cr}$ with time, for the trajectory we have selected, is presented in Fig. 2 for the constant $C_{m_\alpha}$ given previously, and for the Mach-number-dependent $C_{m_\alpha}$ used in the analysis. The difference between the two curves is due to the variation of the term $(C_{m_\alpha} q_\infty)$ throughout the trajectory.

Several hundred runs were made using the analytical roll program, with over 50 verification runs being made using a 6-DOF program. With a few notable exceptions, the roll results of the two programs compared to within 5%. As is usually the case, finding the reason for the exceptions provided most of the material presented in this paper.

In order for a vehicle to exhibit persistent roll resonance, it must have a roll acceleration equal to the rate of change of $p_{cr}$ with time. Since the inflection point of the $p_{cr}$ curve of Fig. 2 occurs at the time of maximum dynamic pressure ($t$ = 35 sec), it was reasoned that the roll-rate change of the vehicle by this time should be a good measure of the effectiveness of a given asymmetry. If the roll-rate is locked-in, the roll rate will equal $p_{cr}$, and the roll-rate change will be 33 rad/sec. If the roll-rate change exceeds 33 rad/sec, the roll acceleration is excessive and the asymmetries causing it are "supercritical."

The change in roll rate of the vehicle for various combinations of the aerodynamic asymmetries is presented in Fig. 3. Note the extreme sensitivity of $\Delta p$ to small differences in $C_{n_0}$ for several of the $C_{m_0}$ curves. The almost discontinuous increase in $\Delta p$ for a small change in $C_{n_0}$, when $C_{m_0} = 0$, corresponds to transient roll lock-in and breakout conditions, where the vehicle rolls up and temporarily matches the slope of the $p_{cr}$ curve. Since the available torque is insufficient to maintain the roll acceleration required for lock-in, the roll breaks out. This type of anomalous roll behavior is illustrated in Fig. 4a, along with a case of persistent roll resonance and a case of supercritical roll-up ahead of the $p_{cr}$ curve.

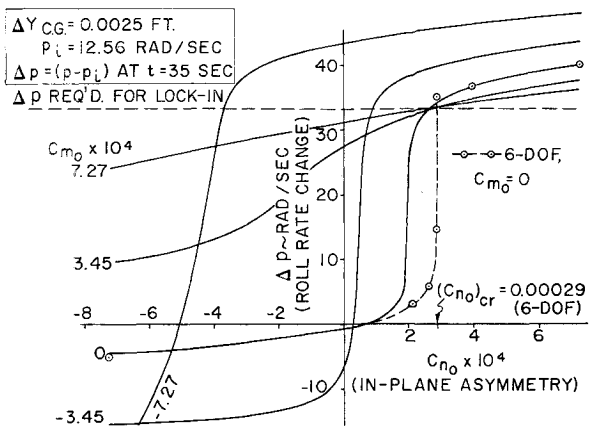


**Fig. 3 Roll-rate change with asymmetry magnitude.**

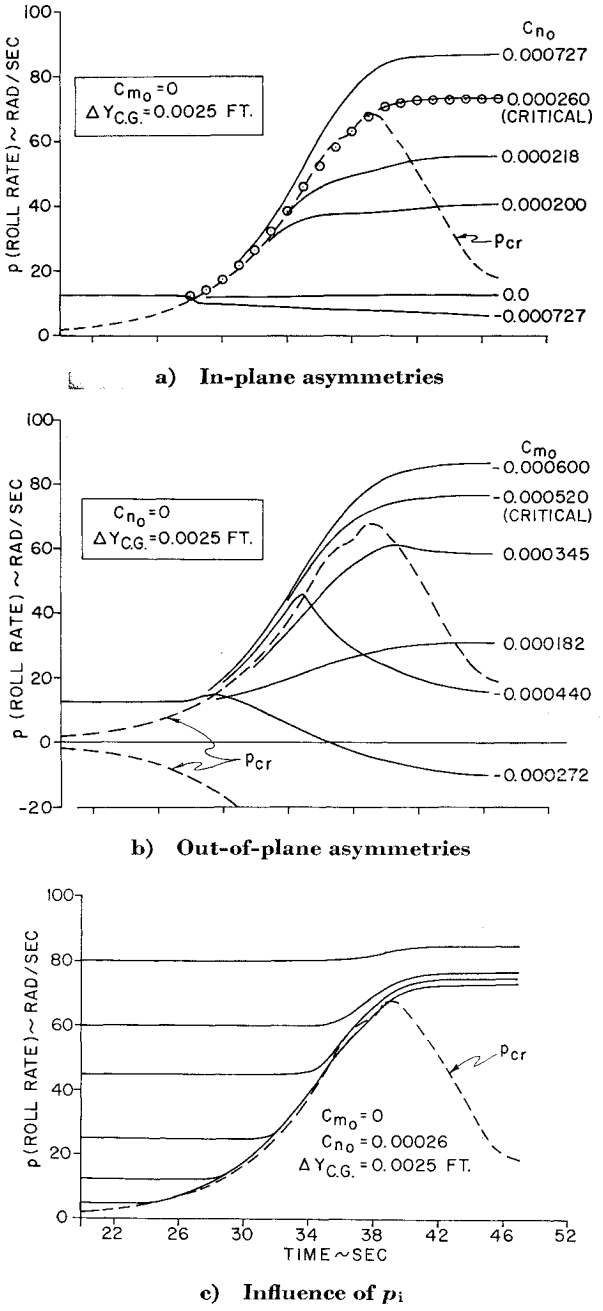


**Fig. 4 Typical roll histories with the analytical program.**

The extremely sensitive asymmetry range with $C_{m_0} = 0$ is confirmed by 6-DOF calculations, as illustrated in Fig. 3. There is excellent agreement between the two programs, except in the extremely sensitive roll breakout region. This lag in the 6-DOF results is due in part to the inertia of a real vehicle, compared to the instantaneous response to trim amplification assumed by the analytical program, and it is due also to the oscillations about trim of a real vehicle which is not considered by the analytical program. The extent of the lag is slightly sensitive to the vehicle attitude and lateral rates at first resonance. It is interesting to note that the 6-DOF results indicate persistent roll resonance with $C_{n_0}$ = 0.000290, which is the point of intersection of the positive $C_{m_0}$ lines of Fig. 3.

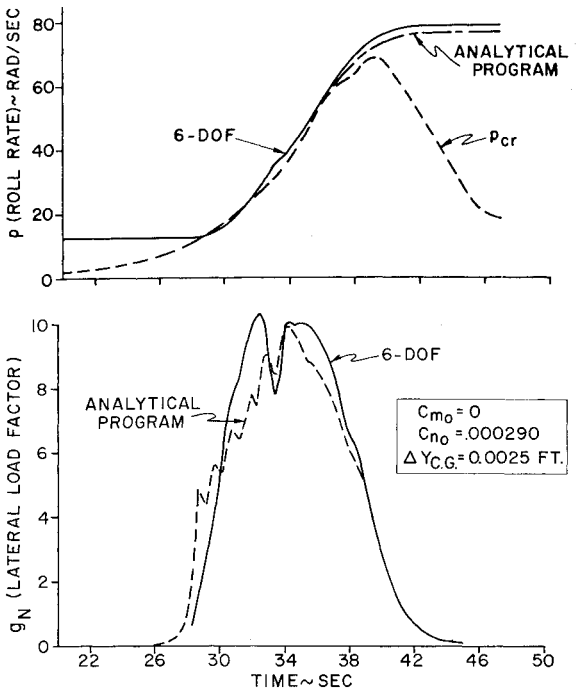


**Fig. 5 Persistent roll resonance time histories of the roll rate and lateral load factor.**

The data of Fig. 3 yield two values for the minimum asymmetry that will cause persistent roll resonance, which is designated as the "critical" in-plane asymmetry. The analytical solution shows that $(C_{n_0})_{cr} = 0.000260$, and the 6-DOF solution shows $(C_{n_0})_{cr} = 0.000290$. The roll-rate time history for the analytical value is presented in Fig. 4a. For purposes of comparison, the analytical roll-rate time history with $C_{n_0} = 0.000290$ is shown along with the 6-DOF history in Fig. 5. Note the ideal response of the roll rate obtained with the analytical program, which closely follows the $p_{cr}$ curve, compared to the slower initial rise of the roll rate obtained with the 6-DOF program. A comparison of the normal load factor histories obtained using the two programs is also presented in Fig. 5. It must be emphasized that much better agreement between the programs is obtained, for all of the pertinent variables, at asymmetry conditions removed from this extremely sensitive region.

An examination of Fig. 3 indicates that it should also be possible to achieve persistent roll resonance with an out-of-plane asymmetry only ($C_{n_0} = 0$). This possibility is examined in Fig. 6, and we see that $\Delta p$ asymptotically approaches the value required for lock-in, with positive $C_{m_0}$, and that very large values of $C_{m_0}$ are required to approach persistent roll resonance. Typical roll-rate histories for positive $C_{m_0}$ are shown in Fig. 4b, and we see that the roll-rate curves are approaching the $p_{cr}$ curve from the underside. The roll rate cannot precisely follow the $p_{cr}$ curve with $\lambda = 1$ and $\beta_0 = 0$, because roll-torque amplification is zero, as pointed out in Refs. 4 and 5.

For negative values of $C_{m_0}$, Fig. 6 shows an extremely sensitive asymmetry range where $\Delta p$ abruptly changes sign and magnitude. This almost discontinuous increase in $\Delta p$ for a small increase in negative $C_{m_0}$ is quite similar to that shown for the in-plane asymmetry. In this case, however, positions along the steep part of the curve correspond to supercritical roll up ahead of the $p_{cr}$ curve, crossover, and then rapid roll down. This type of roll behavior is illustrated in Fig. 4b.

The extremely sensitive asymmetry range with $C_{n_0} = 0$ is confirmed by 6-DOF calculations, as illustrated in Fig. 6, but the response lag is much greater for the out-of-plane asymmetry than it was for the in-plane asymmetry. The lag is also very sensitive to the vehicle attitude and lateral rates at first resonance.

The data of Fig. 6 yields two values for the minimum out-of-plane asymmetry which will produce "supercritical" roll up ahead of the $p_{cr}$ curve that is not followed by rapid roll down. These asymmetries will be designated the "critical" out-of-plane asymmetries. The analytical solution shows that $(C_{m_0})_{cr} = 0.000520$, and the 6-DOF solution shows $(C_{m_0})_{cr} = 0.000580$. The roll-rate history for the analytical value is presented in Fig. 4b. It is interesting to note that these out-of-plane values are exactly twice the magnitude of the critical in-plane asymmetries.

The vehicle roll response to various combinations of the asymmetry moments can also be presented in terms of the resulting trim vector magnitude and orientation. If the drag force and center-of-gravity contribution to the angle of sideslip is neglected, a modified nonrolling trim angle magnitude can be defined as

$$\delta'_0 = [(-C_{m_0}/C_{m_\alpha})^2 + (C_{n_0}/C_{m_\alpha})^2]^{1/2} \quad (23)$$

and its orientation to the $i\alpha$ axis is given by

$$\varphi'_0 = \tan^{-1}(-C_{n_0}/C_{m_0}) \quad (24)$$

The data presented in Fig. 3 can be converted, using the preceding expressions, to show the roll-rate change vs the modified nonrolling trim vector, as presented in Fig. 7. The maximum lateral load factor experienced by the vehicle is presented in Fig. 8. Also shown in these figures is the critical in-plane trim angle ($\delta'_0 = 0.715°$). For trim angles in excess of this minimum value, there are two orientation opportunities for producing persistent roll resonance.

### Anomalous Roll Behavior

The characteristics of the foregoing roll histories can be understood by examining the equations of the linear theory. Three characteristics stand out in particular: 1) very little change in roll rate is experienced until first resonance, 2) in-plane asymmetries produce continuously increasing or decreasing roll rates, depending upon the sign of $C_{n_0}$, and 3) out-of-plane asymmetries produce a reversal of the roll acceleration after the vehicle passes through first resonance.

The first characteristic is explained by examining the trim amplification factor at high altitudes, where $p_{cr}$ and $\mu$ are very small. For these conditions $|R| \approx \lambda^{-2} \ll 1$, and the rolling trim magnitude is much smaller than the nonrolling trim. This fact, coupled with the low dynamic pressure at high altitude, indicates that very little change in roll rate can be expected until $\lambda \to 1$, regardless of the size of the asymmetry.

The other two points are explained by examining the orientation of $\delta_T$ with respect to $\delta_0$, throughout the trajectory. Utilizing Eq. (20), we find that $\delta_T$ leads $\delta_0$ by a angle be-

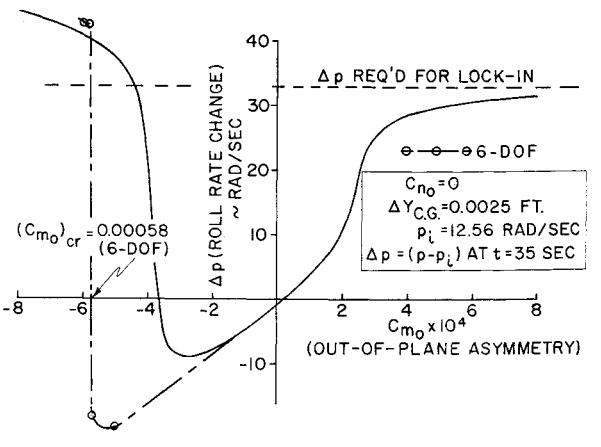


**Fig. 6 Critical out-of-plane aerodynamic asymmetry.**

tween 90 and 180°, as long as $p > p_{cr}$. When $p = p_{cr}$, $\Delta\varphi = 90°$ and $|R| = (2\mu)^{-1}$. When $p < p_{cr}$, $\delta_T$ leads $\delta_0$ by an angle between 0 and 90°. For an in-plane asymmetry, this indicates that the sign of the roll torque will remain constant throughout the trajectory, as shown in Fig. 9. This is a very stable situation that cannot be disturbed significantly by oscillations about the trim due to undamped vehicle motion. For an out-of-plane asymmetry, the vector orientations shown in Fig. 9 shift by 90°, and the sign of the roll torque is dependent upon the magnitude of $p$ with respect to $p_{cr}$. This is an unstable situation that is very sensitive to oscillations about trim. The oscillatory characteristics of the roll rate are dependent upon the initial conditions selected at re-entry; therefore, this type of motion is highly probabilistic. A more detailed discussion of this phenomena is available in Ref. 6. Passive design techniques for avoiding persistent roll resonance, such as deliberately introducing asymmetries to spin the vehicle up ahead of the $p_{cr}$ curve, should seriously consider an in-plane asymmetry in order to avoid this problem.

### Persistent Roll Resonance Criteria

For a center-of-gravity offset taken along the positive $Y$ axis of the vehicle, the maximum roll torque is produced by a rolling trim force which is orthogonal to the $Y$ axis. An examination of Fig. 9 will show that the optimum orientation for lock-in is achieved when $\alpha_0 = 0$, and $\beta_0$ is negative. The lateral force experienced during persistent roll resonance for this optimum orientation is given by

$$F_{z_{res}} = C_{N_\alpha}(\beta_0/2\mu)q_\infty S \tag{25}$$

and the rolling torque is given by

$$l_{x_{res}} = -C_{N_\alpha}(\beta_0 \Delta Y_{c.g.}/2\mu)q_\infty S \tag{26}$$

Using Eq. (26), the maximum roll acceleration available for a given asymmetry magnitude can be written

$$\dot{p}_{res} = (-C_{N_\alpha} q_\infty S/2\mu I_x)(\beta_0 \Delta Y_{c.g.}) \tag{27}$$

Substituting for $\mu$ using Eq. (17), and assuming a constant velocity re-entry yields

$$\dot{p}_{res} = -C_{N_\alpha} V_i p_i(\beta_0 \Delta Y_{c.g.})/\xi \tag{28}$$

where

$$\xi = [C_{N_\alpha}/m - C_{m_q} d^2/2(I - I_x)]I_x \tag{29}$$

For an exponential atmosphere, the density at any altitude can be found using $\rho_\infty = \rho_{si}e^{-\eta h}$, where $\eta$ is the scale height Using this relationship along with Eq. (18), and assuming a constant velocity re-entry with constant aerodynamic coefficients, the rate of change of $p_{cr}$ with time at the point of

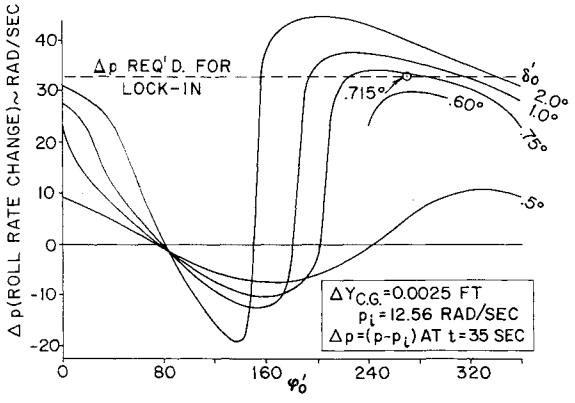


**Fig. 7 Roll-rate change with trim magnitude and orientation.**

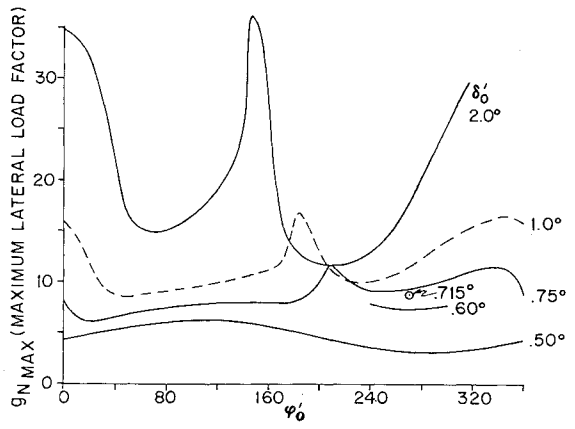


**Fig. 8 Maximum lateral load factor with trim magnitude and orientation.**

first resonance can be shown to be

$$(\dot{p}_{cr})_{res} = -p_i\,(\eta V_i \sin\gamma_i/2) \tag{30}$$

The vehicle acceleration must equal the rate of change of $p_{cr}$, if persistent roll resonance is to occur; therefore, we can equate Eqs. (28) and (30) and solve for the critical compound asymmetry needed to establish persistent roll resonance,

$$(\beta_0 \Delta Y_{c.g.})_{cr} = \xi\eta \sin\gamma_i/2C_{N_\alpha} \tag{31}$$

This criterion, based on constant aerodynamic coefficients, accurately predicted lock-in for 6-DOF simulations with constant coefficients. The critical asymmetry for Mach-number-dependent aerodynamic coefficients also can be predicted by evaluating Eq. (31) with the values of the aerodynamic coefficients at the condition of maximum $q_\infty$. Although Eq. (31) does not directly indicate the influence of initial re-entry velocity or vehicle ballistic coefficient on the critical asymmetry, the influences of these parameters are felt through the aerodynamic coefficients and their variation throughout the trajectory.

The influence of initial roll rate also does not appear in Eq. (31). This implies that the same asymmetry magnitude should cause lock-in regardless of the initial roll rate. To substantiate this point, the initial roll rate was varied between 5 and 80 rad/sec. Figure 4c shows that for initial roll rates smaller than the $p_{cr}$ value at the maximum $q_\infty$ condition (41 rad/sec), the critical in-plane asymmetry determined at a roll rate of 12.56 rad/sec remains unchanged. For initial roll rates larger than 41 rad/sec this asymmetry magnitude is supercritical.

Once the magnitude of $(\beta_0 \Delta Y_{c.g.})_{cr}$ has been established for a particular trajectory, the critical asymmetry moment can be scaled to other values of $\Delta Y_{c.g.}$ and static margin.

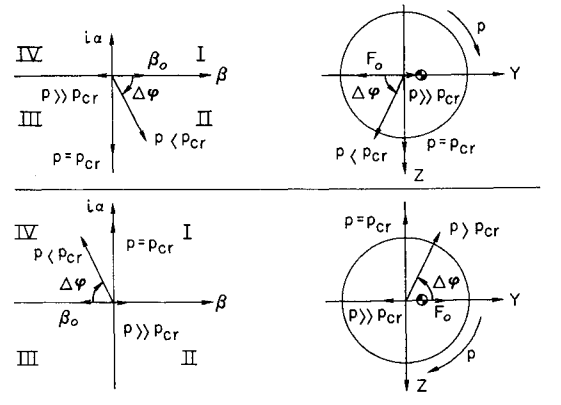


**Fig. 9 Trim orientation and amplification for an in-plane asymmetry.**

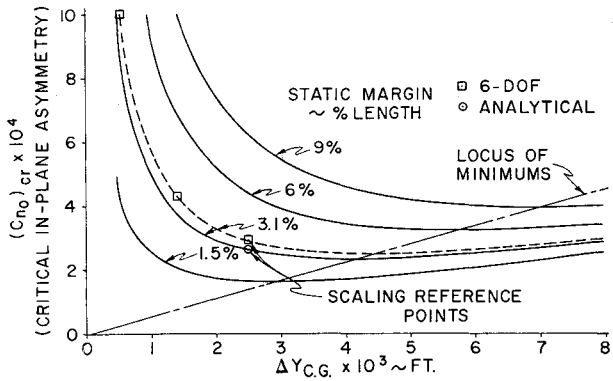


**Fig. 10 Critical in-plane asymmetry with center-of-gravity offset and static margin.**

Results for the vehicle under consideration are presented in Fig. 10. Verification runs were made using 6-DOF simulations for one static margin, with excellent agreement. The analytical program was used to verify the scaling at numerous other conditions.

Each curve in Fig. 10 exhibits a minimum value for the critical in-plane asymmetry. This minimum point can be determined by substituting for $\beta_0$ in Eq. (31), using Eq. (12), solving for $C_{n_0}$, and then determining the minimum value of $C_{n_0}$ by the standard minimum and maximum techniques of differential calculus. The result is

$$(C_{n_0})_{\min} = (-2\xi\eta C_A \Delta X \sin\gamma_i/d^2)^{1/2} \tag{32}$$

and the center-of-gravity offset that this corresponds to is given by

$$(\Delta Y_{c.g.})_{\min} = (C_{n_0})_{\min} d/2C_A \tag{33}$$

An out-of-plane, persistent roll resonance criteria can be obtained in a similar manner. In Ref. 5, Migotsky shows that the maximum roll torque available when $\beta_0 = 0$ is given by

$$l_x = C_{N\alpha}[\alpha_0/4\mu(1 - \mu)]q_\infty S \tag{34}$$

The damping ratio $\mu$ is usually much less than unity and can be neglected; therefore, we can approximate Eq. (34) with

$$l_x = C_{N\alpha}(\alpha_0/4\mu)q_\infty S \tag{35}$$

Comparing this to Eq. (26), we see that this is exactly half the torque that is available from the in-plane asymmetry.

Using the same procedure as before, we arrive at the out-of-plane compound asymmetry that will establish persistent roll resonance

$$(\alpha_0 \Delta Y_{c.g.})_{cr} = \xi\eta \sin\gamma_i/C_{N\alpha} \tag{36}$$

which is just twice as large as the critical in-plane asymmetry given by (31). Comparing the asymmetry moment coefficients, we find that

$$(C_{n_0})_{cr} = -(C_{m_0})_{cr}/2 + C_A \Delta Y_{c.g.}/d \tag{37}$$

The second term of Eq. (37) is usually negligible for small center-of-gravity offsets, so that the critical in-plane asymmetry coefficient is approximately half the magnitude of the out-of-plane coefficient. This explains the results shown in Figs. 3 and 6. For very large values of $\Delta Y_{c.g.}$, however, it is possible for the critical in-plane asymmetry coefficient to be larger than the out-of-plane asymmetry coefficient.

The persistent roll-resonance criteria that are presented in Refs. 4, 5, and 7 are for an out-of-plane compound asymmetry; therefore, the possibility exists that they do not represent the worst conditions.

## Conclusions and Recommendations

A simple, inexpensive, analytical program has been described which provides the analyst with an efficient tool for evaluating the dynamic stability characteristics of a re-entry vehicle having a simple compound asymmetry. This tool can be very useful in design studies to establish manufacturing tolerances.

A typical parametric study using the analytical program and an analysis of the linear theory both indicate that the minimum aerodynamic asymmetry that will cause persistent roll resonance is one which produces a nonrolling force that is directed through the center-of-gravity offset.

A persistent roll resonance criterion has been developed which provides an accurate estimate of the minimum in-plane asymmetry needed for lock-in. The criterion was applied to the results of the parametric study and was found to be very effective.

The analytical approach presented in this paper can be extended to include other mass asymmetries, such as principal axis misalignments and small differences in the pitch and yaw moments of inertia. The effects of asymmetric aerodynamic heating and ablation can be introduced to take into account motion induced asymmetries and their feedback into the motion analysis.

## References

[1] Nicolaides, J. D., "Missile Flight and Astrodynamics," TN-100A, 1959–1961, Bureau of Weapons, Dept. of the Navy.

[2] Glover, L. S., "Effects on Roll Rate of Mass and Aerodynamic Asymmetries for Ballistic Re-Entry Bodies," *Journal of Spacecraft and Rockets*, Vol. 2, No. 2, March–April 1965, pp. 220–225.

[3] Nelson, R. L., "The Motions of Rolling Symmetrical Missiles Referred to a Body-Axis System," TN 3737, Nov. 1956, NACA.

[4] Pettus, J. J., "Persistent Re-Entry Vehicle Roll Resonance," AIAA Paper 66–49, New York, 1966.

[5] Migotsky, E., "On a Criterion for Persistent Re-Entry Vehicle Roll Resonance," AIAA Paper 67–137, New York, 1967.

[6] Barbera, F. J., "An Analytical Technique for Studying the Anomalous Roll Behavior of Ballistic Re-Entry Vehicles," AIAA Paper 69–103, New York, 1969.

[7] Vaughn, H. K., "Boundary Conditions for Persistent Roll Resonance on Re-Entry Vehicles," *AIAA Journal*, Vol. 6, No. 6, June 1968, pp. 1030–1035.